

# DEUTSCHES ELEKTRONEN-SYNCHROTRON **DESY**

DESY 78/77  
December 1978



TESTING QCD: DIRECT PHOTONS IN  $e^+e^-$  COLLISIONS

by

K. Koller

*Sektion Physik, Universität München*

T. F. Walsh

*Deutsches Elektronen-Synchrotron DESY, Hamburg*

P. M. Zerwas

*Deutsches Elektronen-Synchrotron DESY, Hamburg  
and  
Institut für Theoretische Physik, TH Aachen*

NOTKESTRASSE 85 · 2 HAMBURG 52

To be sure that your preprints are promptly included in the  
HIGH ENERGY PHYSICS INDEX,  
send them to the following address ( if possible by air mail ) :

**DESY  
Bibliothek  
Notkestrasse 85  
2 Hamburg 52  
Germany**

Testing QCD: Direct Photons in  $e^+e^-$  Collisions

K. Koller

Sektion Physik, Universität München

T. F. Walsh

Deutsches Elektronen-Synchrotron DESY, Hamburg

P. M. Zerwas

DESY, Hamburg

and

Institut für Theoretische Physik, TH Aachen <sup>+)</sup>

Abstract

We discuss QCD predictions for the production of direct photons in  $e^+e^-$  collisions,  $e^+e^- \rightarrow \gamma^* \rightarrow \gamma + \text{hadrons}$  ( $\mathcal{E} = +$ ). A simple derivation of the QCD results for the structure functions is presented. These turn out to be exactly predicted by the theory, in contrast to hadron production where only the change with  $Q^2$  is predictable. We also take up the phenomenology of this process. A dramatic rise of the  $\gamma/\pi^0$  ratio with  $z = E_\gamma/E_B$  ( $E_\pi/E_B$ ) and with  $Q^2$  is predicted.

<sup>+)</sup>  Permanent address

## I. Introduction

Quantum chromodynamics (QCD) predicts specific patterns of Bjorken scaling violation in deep inelastic scattering /1/ which turn out to be in striking agreement with recent analyses of electromagnetic and weak processes /2/. On a theoretically less rigorous level, it also leads to violations of (Feynman) scaling for the fragmentation functions of quarks and gluons /3/. In the former case, deep inelastic hadron structure functions are concentrated closer and closer to Bjorken  $x = -Q^2/2\nu \rightarrow 0$  as  $-Q^2$  increases; in the latter case, quark and gluon fragmentation functions to hadrons are concentrated closer and closer to Feynman  $z = 2p_{\text{had}} \cdot Q/Q^2 \rightarrow 0$  as  $Q^2 \rightarrow \infty$ , e.g. in  $e^+e^-$  annihilation for  $e^+e^- \rightarrow \pi^0 + \text{anything}$ .

A dramatic change in the conventional picture described above occurs in QCD when one examines the fragmentation function of a quark to a photon (Fig. 1.),

$$e^+e^- \rightarrow \gamma^* \rightarrow \gamma_{\text{DIRECT}} + \text{hadrons} (\mathcal{E} = +) \quad (1)$$

For large  $Q^2$ , direct photon production <sup>+) is dominated by the mechanism where  $\gamma$  is emitted by the quarks before hadron fragmentation due to long range strong interaction forces becomes effective. The contribution from the Born term /4/ drawn in Fig. 2a, to the fragmentation function of the quarks into photons increases as  $\log Q^2$  for  $Q^2 \rightarrow \infty$ . The important feature of QCD is that it predicts a calculable and finite change of the Born term result</sup>

<sup>+) Direct photons are not decay products of radiatively decaying hadrons.</sup>

/5/ for the  $z$  dependent coefficient of  $\log Q^2$  +). This QCD renormalization effect originates in the emission of hard gluons before the photon is radiated (Fig. 2b), all this on a time scale much smaller than the typical time scale of the long range strong interaction forces.

In this paper we will present a simple and transparent derivation of the quark fragmentation functions into photons. So far as we are aware this derivation is new. The main QCD result is due originally to C.H. Llewellyn Smith /5/ who interpreted diagrammatically and extended earlier electron-photon scattering results based on renormalization group techniques by E. Witten /6/. In addition we consider the phenomenology of the process in some detail. Our conclusion is that direct photons in  $e^+e^-$  collisions are measurable. They will afford a new and unique test of QCD. In particular we find a very dramatic rise of the  $\gamma/\pi^0$  ratio with increasing  $z = 2p_T/Q$  and  $Q^2$  ( $\pi^0$  and  $\eta$  provide a background to (1); this background decreases with  $Q^2$  at large  $z$  while (1) increases with  $Q^2$ ).

Section II takes up the derivation of the fragmentation function for (1) in QCD. Section III discusses the phenomenology of  $\gamma$  production in  $e^+e^-$  collisions in some detail. This is necessary because of the background coming from



as well as the Bremsstrahlung background (Fig. 3) from

<sup>+</sup>) This modification is not restricted to QCD, of course; the key is the precise nature of the QCD prediction.

$$e^+e^- \rightarrow \gamma + \gamma^* \quad (3)$$

$$\quad \quad \quad \downarrow$$

$$\quad \quad \quad \text{hadrons } (e = -)$$

It turns out that the background from (3) is nontrivial but appears manageable. It is calculable from  $\sigma(e^+e^- \rightarrow \text{hadrons})$  and can thus be subtracted. In addition, photon-hadron angular correlations are quite different in (1) and (3).

## II. Fragmentation Functions

We begin with a discussion of the structure functions for (1). The cross section reads /4/

$$\frac{d\sigma}{dz d\Omega} = \frac{3\alpha \sigma_{\mu\mu}}{4} z \left[ \bar{W}_T(z, Q^2)(1 + \cos^2\Theta) + \bar{W}_L(z, Q^2)(1 - \cos^2\Theta) \right] \quad (4)$$

where  $z = 2p_f \cdot Q / Q^2 = E_f / E_B$  ( $Q^2 = 4E_B^2$ ),  $\sigma_{\mu\mu} = 4\pi\alpha^2 / 3Q^2$  and  $\Theta$  is the angle between the photon momentum in (1) and the  $e^+e^-$  collision axis.  $\bar{W}_T$  and  $\bar{W}_L$  are transverse and longitudinal structure functions. The Born approximation results for  $\bar{W}_T$  and  $\bar{W}_L$  are (see Fig. 2a) /4/

$$\bar{W}_T^{\text{Born}}(z, Q^2) = \frac{\sum e_q^4}{4\pi^2} \frac{1 + (1-z)^2}{z^2} \log \frac{(1-z)Q^2}{\Lambda^2}$$

$$\bar{W}_L^{\text{Born}}(z, Q^2) = \frac{\sum e_q^4}{\pi^2} \frac{1-z}{z^2} \quad (5)$$

where we have dropped nonleading terms in  $\bar{W}_T^{\text{Born}}$  and have chosen the scale parameter  $\Lambda$  to be the same as we will use later for QCD. (For heavy quarks

we should replace  $\Lambda \rightarrow m_Q$  since the actual parameter in Ref. /4/ is an effective quark mass.) Note that the logarithmic dependence is  $\log(1-z)Q^2/\Lambda^2$ , where the increase with  $Q^2$  originates in the unlimited transverse momentum of the photon relative to the quark jets. It is evident from this that our results are not applicable to events where  $M^2 = (1-z)Q^2$ , the square of the invariant hadron mass, is small (one photon - one jet events for  $z \rightarrow 1$ ). At these values of  $z$  a calculation of the leading log dependence is insufficient. In the following we set  $\log(1-z)Q^2/\Lambda^2 \rightarrow \log Q^2/\Lambda^2$  for all quarks. The error this introduces is negligible at very high  $Q^2$  and  $z \lesssim .8$  or so. At the same level  $\bar{W}_L$  can be neglected. In the leading log approximation it is convenient to introduce the quark to photon fragmentation functions,

$$\frac{1}{\sigma_T} \frac{d\sigma(e^+e^- \rightarrow \gamma + \dots)}{dz} = \sum_q e_q^2 \{ D_q^\gamma(z, Q^2) + D_q^{\gamma^*}(z, Q^2) \} / \sum e_q^2 \quad (6)$$

with the sums running over all flavor and color quantum numbers. We also introduce moments

$$D_q^\gamma(m, Q^2) = \int_0^1 dz z^{m-1} D_q^\gamma(z, Q^2) \quad (7)$$

$D_q^\gamma(z, Q^2)$  includes strong interaction effects which are not taken account of in the Born term (5). This Born contribution to (6) is

$$\begin{aligned} D_q^\gamma(z, Q^2)^{\text{Born}} &= \frac{\alpha}{2\pi} e_q^2 \frac{1+(1-z)^2}{z} \log Q^2/\Lambda^2 \\ &\equiv e_q^2 d^{\text{Born}}(z) t \end{aligned} \quad (8)$$

with  $t = \log Q^2/\Lambda^2$  and moments defined as in (7).

We know how  $D_q^{\text{Born}}$  changes with  $t$ , but what about the exact  $D_q^\delta$  including strong interaction effects induced by QCD? This can be investigated by extending an elegant technique developed by Altarelli and Parisi /7/. Their method involves finding how a fragmentation function changes in going from scale  $t = \log Q^2$  to  $t + dt$ .

The probability of finding a photon in a quark jet changes due to two different mechanisms as  $t$  is raised to  $t + dt$ . (i) The probability to emit a hard gluon before radiating the photon increases by an amount  $\propto \alpha_s(t) dt$  where  $\alpha_s(t) = g_s^2(t)/4\pi$  and  $g_s(t)$  is the running quark-gluon coupling. (This is the mechanism which introduces the  $Q^2$  dependence of quark fragmentation to hadrons /3/.) (ii) The probability of radiating a photon before the strong interactions become effective (the Born term, see equ. (8)) depends explicitly on  $t$ . It increases by an amount  $\propto \alpha dt$  on going from  $t$  to  $t + dt$ . (We do not obtain this sort of contribution for a hadron in a quark jet because of the limited transverse momentum of the hadronization process.) The Born term does not occur for gluon fragmentation to photons. Thus (see fig. 4)

$$\frac{\partial}{\partial t} D_q^\delta(z, t) = e_q^2 d^{\text{Born}}(z) + \frac{\alpha_s(t)}{2\pi} \int_0^1 dx \int_0^1 dy \delta'_1(xy-z) * \quad (9a)$$

$$* \{ D_q^\delta(x, t) P_{qq}(y) + D_G^\delta(x, t) P_{Gq}(y) \}$$

$$\frac{\partial}{\partial t} D_G^\delta(z, t) = \frac{\alpha_s(t)}{2\pi} \int_0^1 dx \int_0^1 dy \delta'_1(xy-z) \left\{ \sum_{q\bar{q}} D_q^\delta(x, t) P_{qG}(y) + \right. \quad (9b)$$

$$\left. + D_G^\delta(x, t) P_{GG}(y) \right\}$$



The functions  $\alpha_s P_{ij}(y)/2\pi$  give the probability for a quantum (quark or gluon)  $j$  to fragment to  $i$  carrying a fraction  $y$  of the original quantum's momentum <sup>†</sup>);  $i$  then fragments further into the observed  $\gamma$  and unobserved hadrons. Equations (9) can be solved by taking moments of both sides. (9) then becomes a system of linear inhomogeneous differential equations. To simplify matters further, we define the sum and difference of the fragmentation functions to  $\gamma$  of charge  $2/3$  and  $-1/3$  quarks

$$D_+^{\delta}(m,t) = \sum_q \int_0^1 dz z^{m-1} D_q^{\delta}(z,t) \quad (10)$$

$$D_-^{\delta}(m,t) = \int_0^1 dz z^{m-1} \{ D_u^{\delta}(z,t) - D_d^{\delta}(z,t) \}, \text{ etc.}$$

and

$$D_G^{\delta}(m,t) = \int_0^1 dz z^{m-1} D_G^{\delta}(z,t) \quad (11)$$

The moments of the functions  $P_{ij}(y)$ ,

$$A_{ij} = \int_0^1 dy y^{m-1} P_{ij}(y) \quad (12)$$

can be found in the literature; they are /3/, /7/

<sup>†</sup>) It is necessary to define  $P_{ij}(y)$  carefully at  $y \rightarrow 1$  so as to get a physically sensible result; for details see Ref. /7/.

$$A_{qq}(m) = -\frac{2}{3} \left[ 1 - \frac{2}{m(m+1)} + 4 \sum_{j=2}^m \frac{1}{j} \right]$$

$$A_{Gq}(m) = \frac{4}{3} \frac{m^2 + m + 2}{m(m^2 - 1)} \quad (13)$$

$$A_{qG}(m) = \frac{1}{2} \frac{m^2 + m + 2}{m(m+1)(m+2)}$$

$$A_{GG}(m) = -\frac{3}{2} \left[ \frac{1}{3} - \frac{4}{m(m-1)} - \frac{4}{(m+1)(m+2)} + 4 \sum_{j=2}^m \frac{1}{j} + \frac{2N_F}{9} \right]$$

with  $N_F$  being the number of quark flavors. For large  $t$  the running coupling constant goes to zero as  $\alpha_s(t) = 1/bt$  with  $2\pi b = (33 - 2N_F)/6$ . It is therefore convenient to define

$$d_m^{qq} = -\frac{1}{2\pi b} A_{qq}(m) > 0 \quad d_m^{Gq} = -\frac{1}{2\pi b} A_{Gq}(m) < 0$$

$$d_m^{qG} = -\frac{1}{2\pi b} A_{qG}(m) > 0 \quad d_m^{GG} = -\frac{2N_F}{2\pi b} A_{GG}(m) < 0 \quad (14)$$

Introducing  $s = \log t/t_0$  with  $t_0 = \log Q_0^2/\Lambda^2$  we now write the equations for the moments as

$$\frac{\partial}{\partial s} D_{-}^{\dagger}(m, s) = \frac{1}{3} t_0 e^s d^{Bom}(m) - d_m^{qq} D_{-}^{\dagger}(m, s) \quad (15)$$

and

$$\frac{\partial}{\partial s} D_{+}^{\dagger}(m, s) = \frac{5N_F}{18} t_0 e^s d^{Bom}(m) - d_m^{qq} D_{+}^{\dagger}(m, s) - d_m^{Gq} D_G^{\dagger}(m, s) \quad (16)$$

$$\frac{\partial}{\partial s} D_G^{\dagger}(m, s) = -N_F^{-1} d_m^{qG} D_{+}^{\dagger}(m, s) - d_m^{GG} D_G^{\dagger}(m, s)$$

The solutions of (15) and (16) are the sum of a general solution of the homogeneous equations and a particular solution of the inhomogeneous equations. The homogeneous part of (15) and (16) is solved by

$$D_{-}^{\delta}(m,s)_{\text{HOMOGENEOUS}} \propto e^{-d_m^{qq} s} \quad (17)$$

$$D_{+}^{\delta}(m,s), D_G^{\delta}(m,s)_{\text{HOMOGENEOUS}} = \text{linear combinations of } e^{\lambda_{\pm} s} \text{ and } e^{\lambda_{-} s}$$

where  $-d_m^{qq} < 0$  and

$$2\lambda_{\pm} = -(d_m^{qq} + d_m^{GG}) \pm \left[ (d_m^{qq} + d_m^{GG})^2 + 4d_m^{Gq} d_m^{qG} \right]^{\frac{1}{2}} \quad (18)$$

$$\leq 0 \text{ for } m \geq 2 \quad [\text{only } \lambda_{+}(m=2) = 0]$$

Thus the solution of the homogeneous equations either vanish asymptotically as negative powers of  $\log Q^2/\Lambda^2$  ( $n > 2$ ) or remain constants ( $n = 2$ ); they can be ignored, as we will now show. (This piece, of course, contains the "hadronic" component of the photon and may well be important at low  $Q^2$ ).

We now have to find the solutions of the inhomogeneous equations (15) and (16). Making the obvious ansatz

$$D_i^{\delta}(m,s) = C_i e^s \text{ for } i = \pm, G \quad (19)$$

we can solve for  $C_{\pm}$  and  $C_G$  after a negligible amount of algebra. The result can be expressed by undoing (10) as

$$D_q^{\gamma}(m, Q^2) = \left[ \left(1 - \frac{5}{18} \frac{1}{e_q^2}\right) \frac{1}{1+d_m^{qq}} + \frac{5}{18} \frac{1}{e_q^2} \frac{1+d_m^{GG}}{K_m} \right] D_q^{\gamma}(m, Q^2)^{\text{Born}} \quad (20)$$

$$D_G^{\gamma}(m, Q^2) = \frac{5}{18} \frac{1}{e_q^2} \frac{d_m^{qG}}{K_m} D_q^{\gamma}(m, Q^2)^{\text{Born}}$$

where

$$K_m = 1 + d_m^{qq} + d_m^{GG} + d_m^{qq} d_m^{GG} - d_m^{Gq} d_m^{qG}$$

Equation (20) is just the result cited in Ref. /5/. We see that (19), (20) dominate at large  $Q^2$ . The homogeneous solution can be neglected.

In order to convert this expression for the moments into  $D_q^{\gamma}(z, Q^2)$  we need to invert the moment integrals. This is conventionally done on a computer by the Mellin method and a numerical result was presented by C.H. Llewellyn Smith /5/. The ratio

$$F_q(z) = D_q^{\gamma}(z, Q^2) / D_q^{\gamma}(z, Q^2)^{\text{Born}} \quad (21)$$

(where  $D_q(z, Q^2)^{\text{Born}}$  is given in (8)) measures the strength of the QCD renormalization effects; the result for  $F_q(z)$  is shown in Fig. 5.

At the end of this Section a word about the physical meaning of the QCD analysis is in order. (i) There is a striking difference between the  $Q^2$  evolution of hadron spectra and photon spectra in quark jets. This originates in the Born term contribution with unlimited transverse momentum in the

photon case. Moments of hadron spectra fall monotonically to zero for  $Q^2 \rightarrow \infty$ , whereas the QCD term rises as  $\log Q^2$  and finally dominates the photon spectra. (ii) The Born term describes the probability of order  $\alpha \log Q^2$  that a quark produced in  $e^+e^-$  (or anywhere else) will immediately radiate a hard photon. But the quark can also radiate  $n$  hard gluons each with probability of order  $\alpha_s \log Q^2$ , before radiating the hard photon. Summing over this series of  $(\alpha \log Q^2) (\alpha_s \log Q^2)^n$  damps hard photon radiation by a finite factor because  $\alpha_s \propto (\log Q^2)^{-1}$  asymptotically. So even after QCD renormalization we are left with an exactly predictable, leading  $\log Q^2$  term in the quark fragmentation functions to photons. By contrast, only the change with  $Q^2$  of the fragmentation functions is predicted by QCD for hadron production in  $e^+e^-$  annihilation.

### III. Phenomenology

This Section consists of the answers to a number of evident questions which have to be put before concluding that reaction (1) can be used to test QCD.

#### 1) Rates and Approximations

We have ignored the longitudinal structure function in (4); neglecting QCD corrections to both  $\bar{W}_T$  and  $\bar{W}_L$  for the moment we estimate from (5)

$$\frac{\bar{W}_L}{\bar{W}_T} \sim \frac{4(1-z)}{1+(1-z)^2} \frac{1}{\log Q^2/\Lambda^2} \lesssim 0.2 \quad (22)$$

for  $z \gtrsim 1/2$ ,  $Q^2 \sim 10^3 \text{ GeV}^2$  and  $\Lambda \sim 400 \text{ MeV}$ . Our approximation is clearly

acceptable for large  $z$ . Given enough data, one can even imagine separating  $\bar{W}_T$  and  $\bar{W}_L$  via the angular dependence in (4).

We ignored the fact that the argument of the log in (5) is not  $Q^2$  but  $M^2 = (1-z)Q^2$  and that for heavy quarks, e.g. charm,  $\Lambda^2 \rightarrow m_Q^2$ . Separately neither of these effects changes  $\bar{W}_T$  by more than  $\mathcal{O}(20\%)$  if  $z \leq .8$ , and they reduce the cross section whereas (22) increases it.

Finally we estimate the ratio of the inclusive  $\gamma$  rate to the total cross section  $\sigma_{TOT} = \sum e_q^2 \sigma(e^+e^- \rightarrow \mu^+\mu^-)$ . For charge  $2/3$  quarks,

$$\frac{1}{\sigma_{n\bar{u}} + \sigma_{c\bar{c}}} \int_{z_{min}}^{z_{max}} dz \frac{d\sigma(\gamma n\bar{u} + \gamma c\bar{c})}{dz} = \frac{4}{9} \frac{\alpha}{\pi} \log \frac{Q^2}{\Lambda^2} \int_{0.5}^{0.8} dz \frac{1+(1-z)^2}{z} F_{2/3}(z) \quad (23)$$

$$\sim .005 \text{ at } Q^2 \sim 10^3 \text{ GeV}^2; \Lambda \sim 400 \text{ MeV}$$

i.e. about 1 in 200 events will contain a hard direct photon with  $.5 \leq z \leq .8$ . (The reason for this choice of limits will become clear shortly.) Thus we expect the process (1) to be measured if a sample of  $\mathcal{O}(10^4)$   $e^+e^-$  events is available.

(ii) The Hadronic Component of the Photon

The leading  $\log Q^2$  term in the fragmentation functions of quarks to photons corresponds only to the pointlike coupling of the photons to quarks. Direct photons can be produced through a hadronic ( $\rho^0$ ) component as in Fig. 6.

We estimate this as follows. VDM relates  $e^+e^- \rightarrow \gamma_{had} + \dots$  to  $e^+e^- \rightarrow \rho^0 + \dots$

Using the experimental fact that  $d\sigma(\rho^0) \approx \lambda d\sigma(\pi^0)$  for large  $z$  where

$\lambda$  is roughly  $z$  independent and of order 1-2, one arrives at

$$\begin{aligned} \frac{1}{\sigma_{\text{TOT}}} \frac{d\sigma(\gamma_{\text{VDM}})}{dz} &\approx \left(\frac{e}{f_9}\right)^2 \lambda \frac{1}{\sigma_{\text{TOT}}} \frac{d\sigma(\pi^0)}{dz} \\ &= \frac{\lambda}{300} \frac{1}{\sigma_{\text{TOT}}} \frac{d\sigma(\pi^0)}{dz} \end{aligned} \quad (24)$$

Essentially, this states that the hadronic component is irrelevant provided the predicted ratio  $\gamma_{\text{QCD}}/\pi^0 \gg 1\%$ . We thus turn next to the  $\gamma/\pi^0$  ratio.

### (iii) The $\gamma/\pi^0$ Ratio

We consider this quantity for two reasons. First,  $\pi^0$  (and  $\eta$ ) mesons decay to  $\gamma\gamma$  and these photons can be confused with the direct photons we are interested in. A separation is possible only if the ratio of direct photons to  $\pi^0$  at the same momentum is not too small. The second reason is the estimate of the "hadronic" part of the photon yield described above. (In addition, the  $\gamma/\pi^0$  ratio can be used to compare different experiments of uncertain relative normalization).

The  $\gamma/\pi^0$  ratio as a function of  $z$  and  $Q^2$  is calculated under the following assumptions. A satisfactory parametrization for the  $\pi^0$  fragmentation function of u and d quarks at  $Q_0^2 = 25 \text{ GeV}^2$  is provided by

$$z D_{u,d}^{\pi^0}(z, Q_0^2) = A (1-z)^2 \quad (25)$$

Adopting the fits of Ref. /8/ we choose  $A = 0.5$ . (This is not inconsistent with DASP data on  $e^+e^- \rightarrow \pi^\pm + \dots$  at  $z \gtrsim .5$ , the range we are interested in).

The  $s, \bar{s}$  quark fragmentation functions are assumed to fall off faster to zero for  $z \rightarrow 1$  (see /8/),

$$D_s^{\pi^0}(z, Q_0^2) / D_{u,d}^{\pi^0}(z, Q_0^2) = (1-z)/(1+z) \quad (26)$$

We estimate the  $\pi^0$  yield of fragmenting charmed quarks by using the same ansatz (26) at  $Q_0 = 5$  GeV. Since we are studying the  $\gamma/\pi^0$  ratio at very large  $Q^2$  of the order of  $10^3$  GeV<sup>2</sup> we must take scaling violations in the quark fragmentation functions to pions into account. The  $Q^2$  evolution of these functions is governed by a set of master equations identical to the homogeneous parts of (9) with the replacement  $\gamma \rightarrow \pi^0/3$ . Into the solution of these equations enters the gluon fragmentation function at  $Q_0^2$  (chosen as  $25$  GeV<sup>2</sup>) which we assume to be equal to the singlet SU(3) quark fragmentation function

$$D_G^{\pi^0}(z, Q_0^2) = \frac{1}{3} (D_u^{\pi^0} + D_d^{\pi^0} + D_s^{\pi^0})(z, Q_0^2) \quad (27)$$

The evolution equations are solved by employing the same methods as described for the  $\gamma$  case. The results for  $D_{u,d}^{\pi^0}(z, Q^2), D_{s,c}^{\pi^0}(z, Q^2)$  are shown in Fig. 7a to b at  $Q^2 = 25, 100, 1000$  and  $10,000$  GeV<sup>2</sup>. The ratio of QCD  $\gamma$ 's over  $\pi^0$ 's is now given as

$$\frac{d\sigma(\gamma_{\text{ACO}})/dz}{d\sigma(\pi^0)/dz} = \frac{\alpha}{\pi} \log \frac{Q^2}{\Lambda^2} \frac{\frac{1+(1-z)^2}{z} \left[ \frac{3z}{81} F_{2/3}(z) + \frac{z}{81} F_{1/3}(z) \right]}{\frac{2}{9} D_{2/3}^{\pi^0}(z, Q^2) + \frac{z}{9} D_{1/3}^{\pi^0}(z, Q^2)} \quad (28)$$

with  $D_{2/3} = D_u + D_c$  and  $D_{1/3} = D_d + D_s$ . We have plotted eq. (28) as a function of  $z$  for  $Q^2 = 100$  GeV<sup>2</sup>,  $1000$  GeV<sup>2</sup> and  $10,000$  GeV<sup>2</sup>. In Fig. 8 we want to call attention to the dramatic rise of  $\gamma/\pi^0$  with  $z$  and  $Q^2$ . That this



ratio  $\gamma_{had} / \pi^0 \gg 1\%$  for  $z \gtrsim .5$ , justifies a posteriori our neglect of any hadronic component to the photon (see eq. (24)).

(iv) The Bremsstrahlung Process

A significant background to (1) arises from (3), where the photon is radiated from an initial line rather than from a final quark line. Whereas on general grounds the cross sections for both reactions are expected to be of comparable magnitude, the photon and quark jets predominantly populate quite different regions of phase space. Photons of the bremsstrahlung process (1) are preferentially emitted into a narrow cone around the lepton beam axis; there is no strong angular correlation between the photon direction and quark jet directions (apart from energy-momentum conservation). By contrast, photons emitted from a quark in the final state are not strongly correlated with the  $e^+e^-$  beam axis; we expect, however, the opening angle between the photon and quark jets to be small on the average (the relative transverse momentum is of course not limited but grows indefinitely with energy). This can be made quantitative by comparing the cross section for  $e^+e^- \rightarrow q\bar{q} \rightarrow q\bar{q}\gamma$  and  $e^+e^- \rightarrow \gamma\gamma^* \rightarrow \gamma q\bar{q}$  in the Born term approximation. Denoting the fraction of beam energy transferred to the  $q$  and  $\bar{q}$  jet by  $x_q$  and  $x_{\bar{q}}$  and the angle between  $\gamma$  and the  $q(\bar{q})$  jet by  $\theta_{\gamma q}$  ( $\theta_{\gamma \bar{q}}$ ) we obtain

$$\frac{1}{\sigma_{\mu\mu}} \frac{d\sigma(\gamma_{DIRECT})}{dz dx_q d\cos\theta} = \frac{3\alpha \sum e_q^4}{16\pi} \frac{B}{(1-x_q)(1-x_{\bar{q}})} \quad (29a)$$

$$\frac{1}{\sigma_{\mu\mu}} \frac{d\sigma(\gamma_{BREMS})}{dz dx_q d\cos\theta} = \frac{3\alpha \sum e_q^4}{4\pi} \frac{B}{z^2(1-z)(1-\cos^2\theta)} \quad (29b)$$

with 
$$B = (x_q^2 + x_{\bar{q}}^2 - x_1^2)(1 + \cos^2 \theta) + 2 \sin^2 \theta x_1^2$$

and 
$$x_1^2 = 4(1-z)(1-x_q)(1-x_{\bar{q}})/z^2$$

$$z + x_q + x_{\bar{q}} = 2$$

$$x_q(1 - \cos \theta_{\gamma q}) = 2(1 - x_{\bar{q}}) \quad \text{and} \quad q \leftrightarrow \bar{q} \tag{30}$$

following from energy momentum conservation. Contributions from  $\gamma$  emission by the leptons are smallest if the hard photon rays are observed under  $90^\circ$  to the beam axis and  $z$  is not too close to 1. For this configuration the cross sections (29a) and (29b) are shown in Fig. 9 as functions of the angle between photon and quark/antiquark jets for  $z = .7$ . The strong ( $\gamma$  quark) correlation enables us to separate the direct photons sufficiently well from the Bremsstrahlung background (given in a model independent way by replacing  $\sum e_q^2 \rightarrow R(M^2) = \sigma_{TOT}(e^+e^- \rightarrow \text{hadrons}) / \sigma(e^+e^- \rightarrow \mu^+\mu^-)$  in (29b),  $M^2 = (1-z)Q^2$ ).

#### IV. Conclusions

We have discussed in detail direct photon production in  $e^+e^-$  collisions,  $e^+e^- \rightarrow \gamma + \text{hadrons}$  ( $\mathcal{E} = +$ ). This reaction appears to be a quite intriguing test of quantum chromodynamics. Unlimited transverse momentum in photon radiation off quarks makes the shape of photon spectra in quark jets quite different from hadron spectra, as well as the pattern of scaling violations in the fragmentation functions. The asymptotic form of the quark fragmentation functions to photons is predictable in QCD and we have presented a simple and transparent derivation by defining a set of (inhomogeneous) master equations for the energy evolution of the photon spectra. In this context the behavior

of the  $\gamma/\pi^0$  ratio is particularly instructive as it arises from the logarithmic increase of the  $\gamma$  yield combined with the logarithmic decrease of the  $\pi^0$  yield. The yield of hard direct photons at PETRA and PEP is expected to be larger than the  $\pi^0$  yield. Experimental tests of these QCD predictions would be most welcome.

#### Acknowledgement

K.K. and P.M.Z. thank H. Joos and T.F. Walsh for the kind hospitality extended to them at DESY. K.K. acknowledges discussions with H. Salecker and his interest in this work.

References

- /1/ H.D. Politzer, Phys. Rep. 14C (1974) 129;  
O. Nachtmann, Proc. Hamburg Conf. 1977
  
- /2/ H.L. Anderson et al., Phys. Rev. Letters 40 (1978) 1061;  
P.C. Bosetti et al., Nucl. Phys. B142 (1978) 1
  
- /3/ J.F. Owens, Phys. Letters 76B (1978) 85;  
T. Uematsu, Kyoto preprint;  
R.P. Feynman, R.D. Field and G.C. Fox, Caltech preprint CALT-68-651
  
- /4/ T.F. Walsh and P. Zerwas, Phys. Letters 44B (1973) 195
  
- /5/ C.H. Llewellyn Smith, Oxford preprint, Ref. 56/78
  
- /6/ E. Witten, Nucl. Phys. B120 (1977) 189
  
- /7/ G. Altarelli and G. Parisi, Nucl. Phys. B126 (1977) 298
  
- /8/ L.M. Sehgal, Proc. Hamburg Conf. 1977

Figure Captions

Fig. 1. Direct production of photons in  $e^+e^-$  collisions. The accompanying hadrons have charge conjugation  $C = +$ . The observed photons are assumed not to be radiative decay products of  $\pi^0, \eta$  etc.

Fig. 2. Photon radiation off quarks:

(a) Born term,

(b) gluonic QCD correction.

Fig. 3. Photon Bremsstrahlung off electrons and positrons.

Fig. 4.  $Q^2$  evolution of quark fragmentation functions to photons: contribution of the Born term and from gluon radiation.

Fig. 5. Ratio  $F_q(z)$  of the QCD renormalized quark fragmentation functions into photons to the Born term, for quark charges  $2/3$  and  $1/3$ .

Fig. 6. Hadronic component of the photon in semiinclusive spectra. This component shows the characteristic features of hadron production, limited transverse momentum relative to the jet axis, etc.

Fig. 7.  $\pi^0$  fragmentation functions at  $Q^2 = 25, 100, 1000$  and  $10,000 \text{ GeV}^2$  for  $u, s$  quarks.

Fig. 8. Ratio of directly produced  $\gamma$ 's to  $\pi^0$ 's at  $Q^2 = 100, 1000$  and  $10,000 \text{ GeV}^2$ .

Fig. 9. Cross sections for direct photon production (Born approximation) and bremsstrahlung from the leptons as a function of the angle between  $\vec{q}$  and the  $q$  or  $\bar{q}$  jet;  $z$  is chosen as 0.7 and the photon flight direction perpendicular to the  $e^+e^-$  axis.

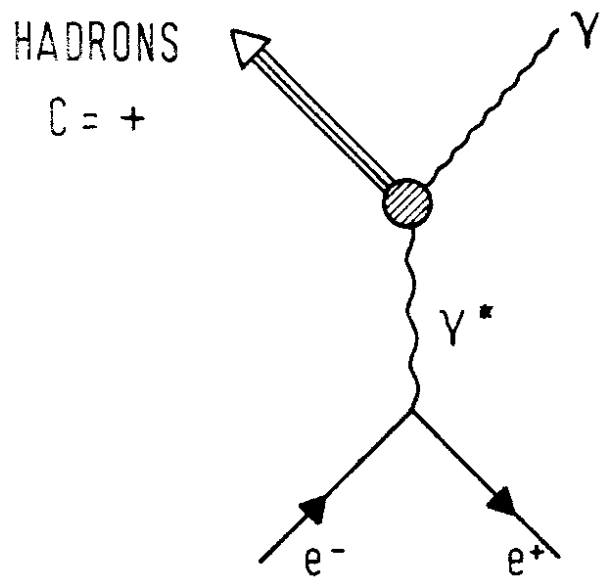


Fig.1

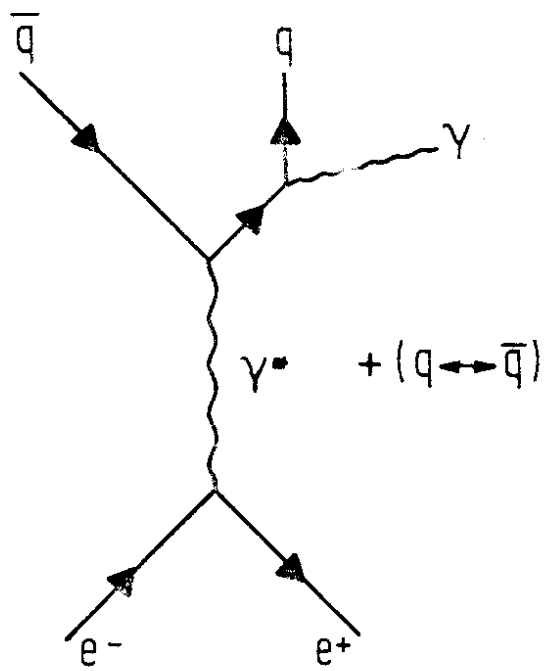


Fig. 2a.

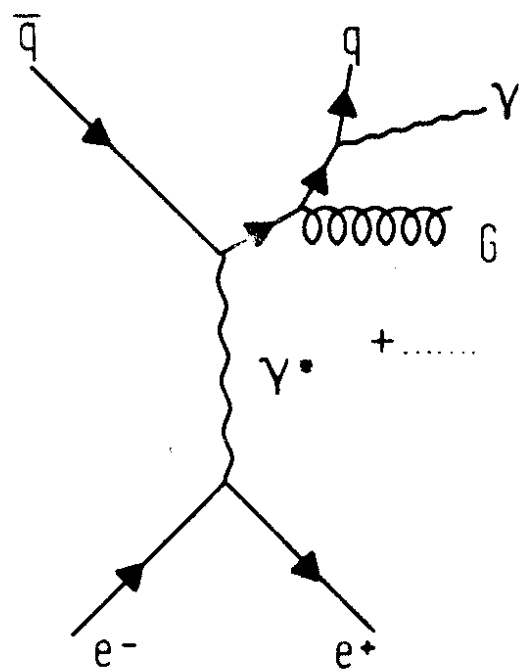


Fig. 2b.

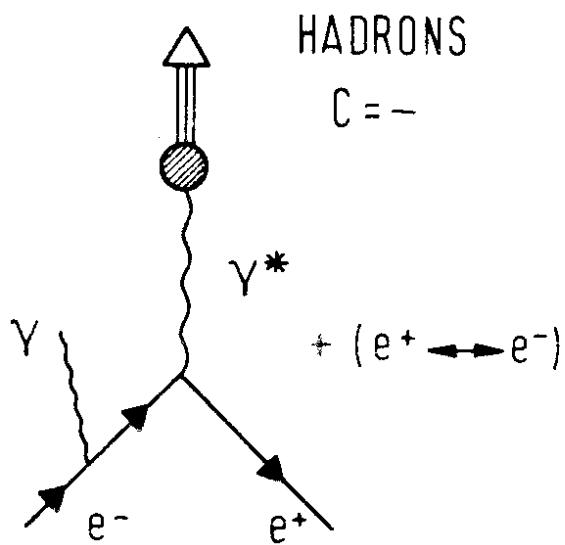


Fig. 3

$$\frac{d}{dt} \left\{ \text{diagram 1} \right\} = \frac{d}{dt} \left\{ \text{diagram 2} \right\} + \left\{ \text{diagram 3} + \text{diagram 4} \right\}$$

The diagrams in the equation represent different interaction topologies:

- Diagram 1:** A quark line (q) enters from the left, hits a shaded vertex, and then splits into a photon (gamma) and a hadron (shaded circle with arrow).
- Diagram 2:** A quark line (q) enters from the left, hits a shaded vertex, and then splits into a quark (q) and a hadron (shaded circle with arrow). A photon (gamma) is emitted from the quark line.
- Diagram 3:** A quark line (q) enters from the left, hits a shaded vertex, and then splits into a quark (q) and a hadron (shaded circle with arrow). A gluon (G) is emitted from the quark line, which then splits into a photon (gamma) and a quark (q).
- Diagram 4:** A quark line (q) enters from the left, hits a shaded vertex, and then splits into a quark (q) and a hadron (shaded circle with arrow). A gluon (G) is emitted from the quark line, which then splits into a photon (gamma) and a quark (q).

Fig. 4



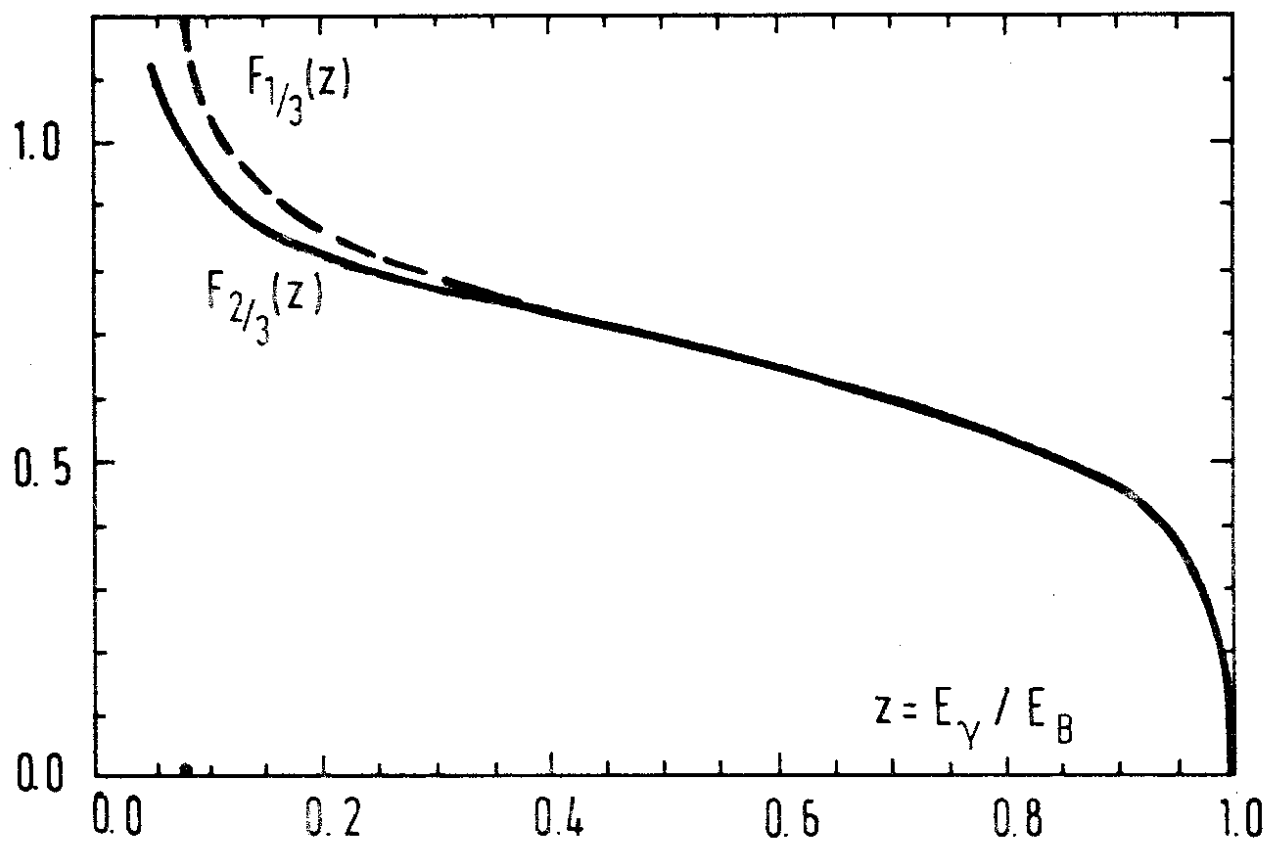


Fig. 5

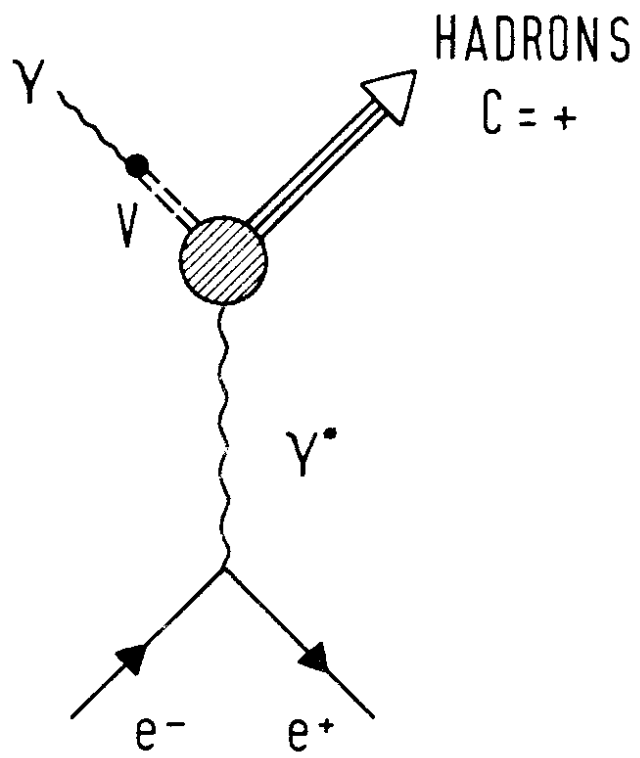


Fig 6

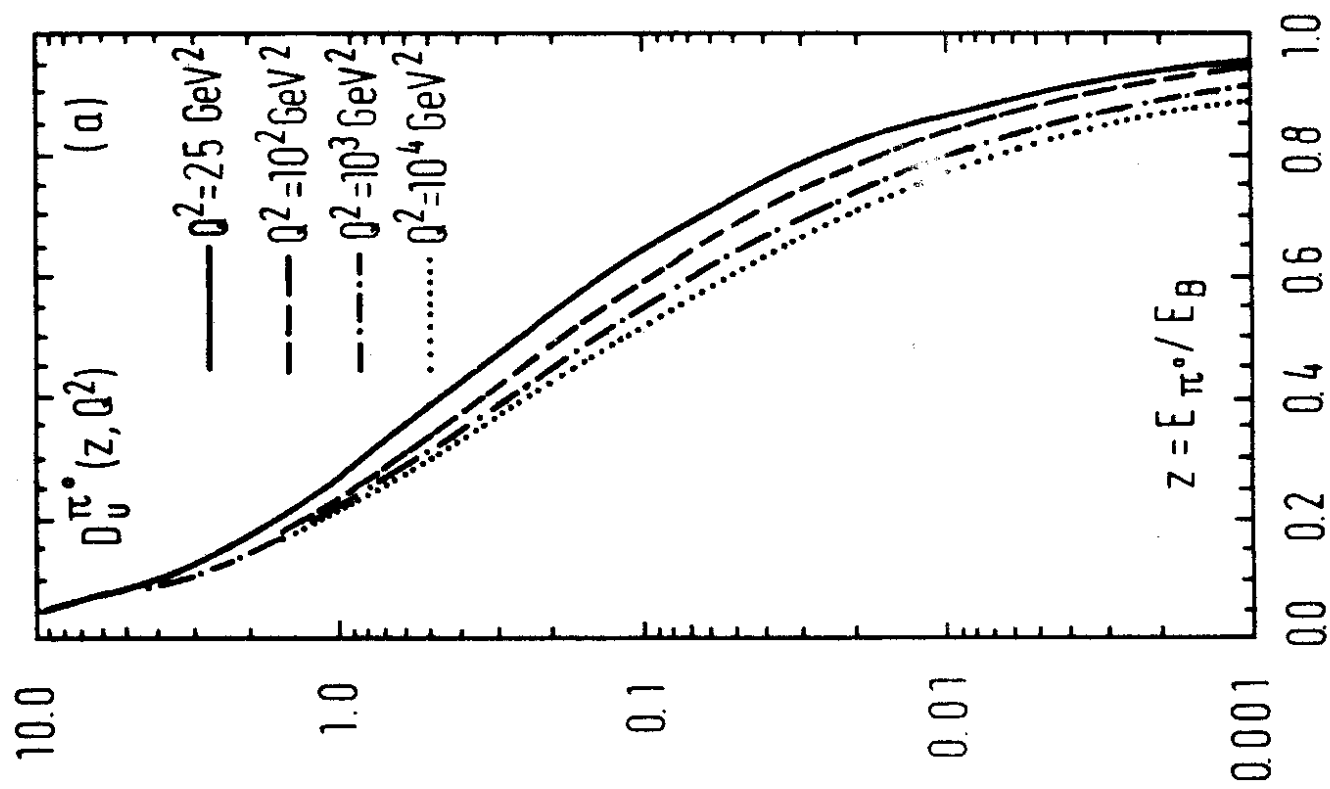
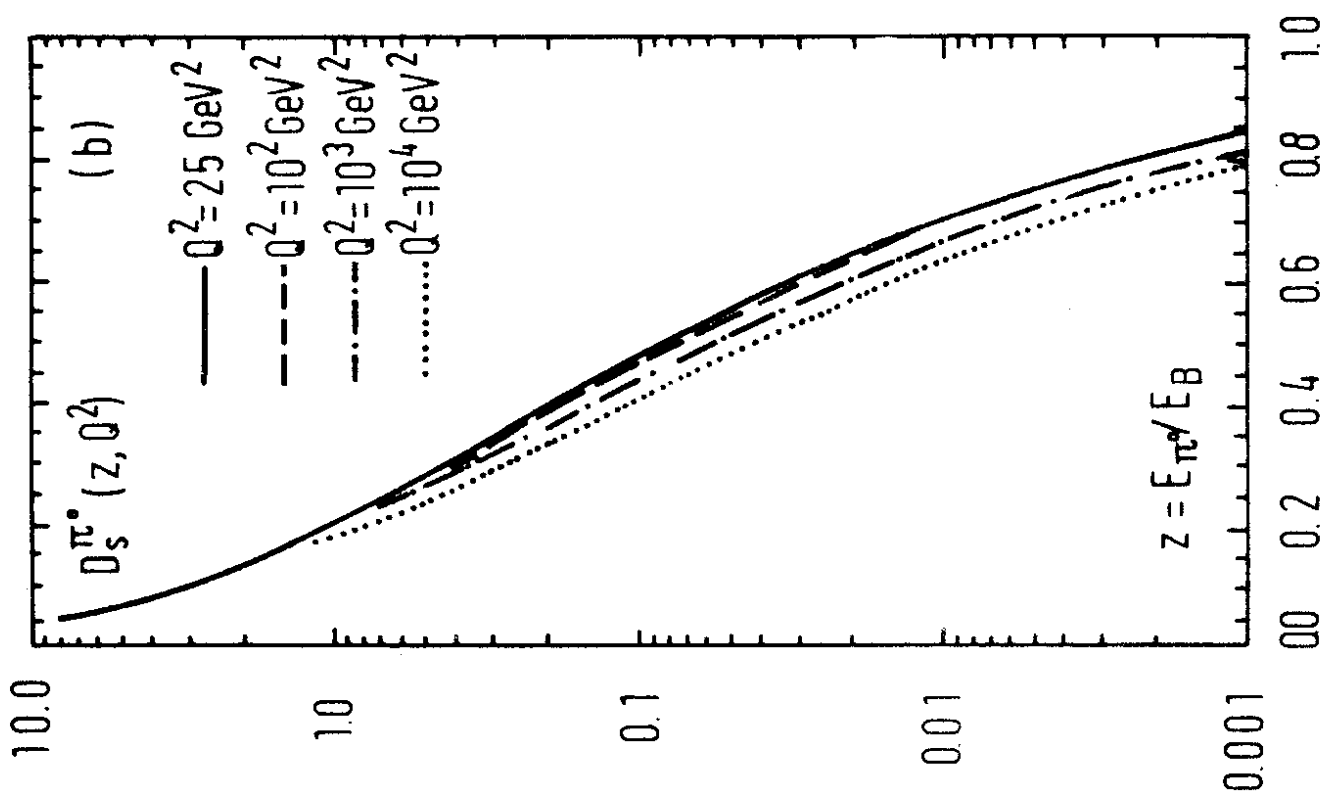


Fig.7

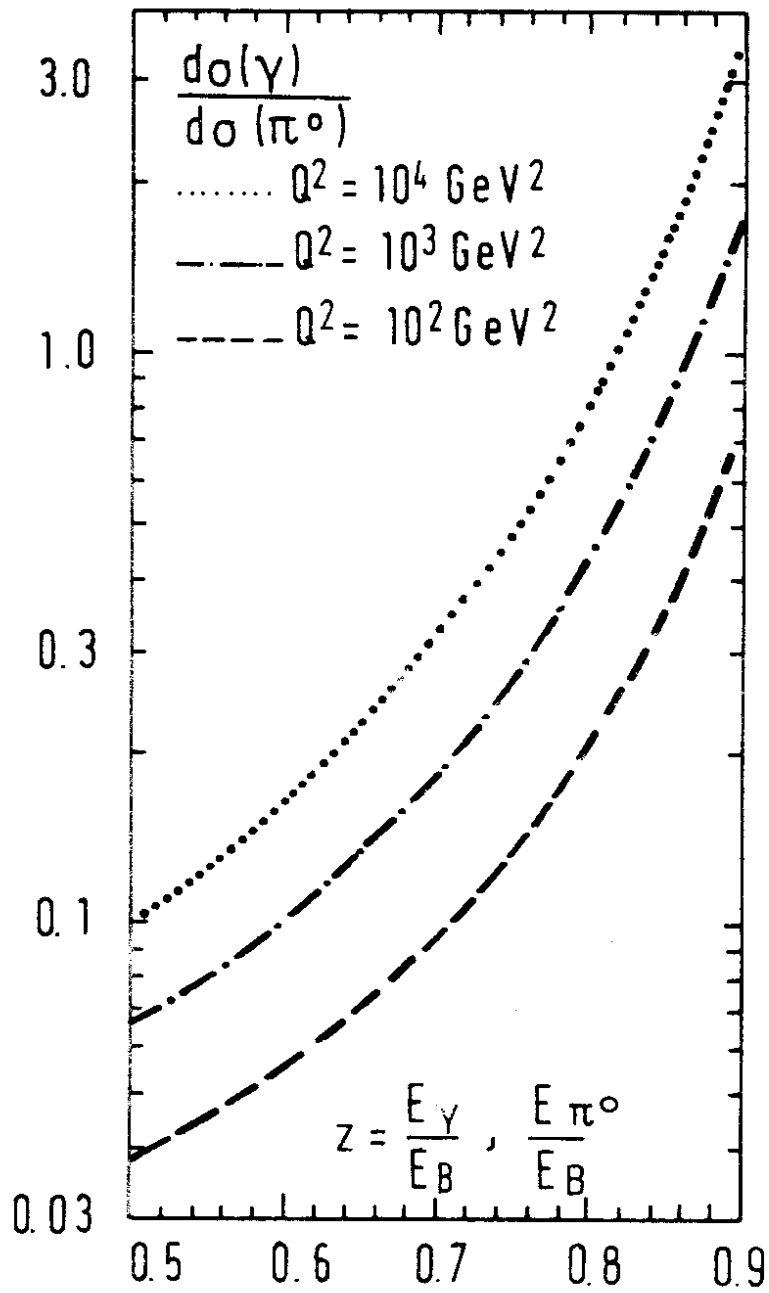


Fig. 8

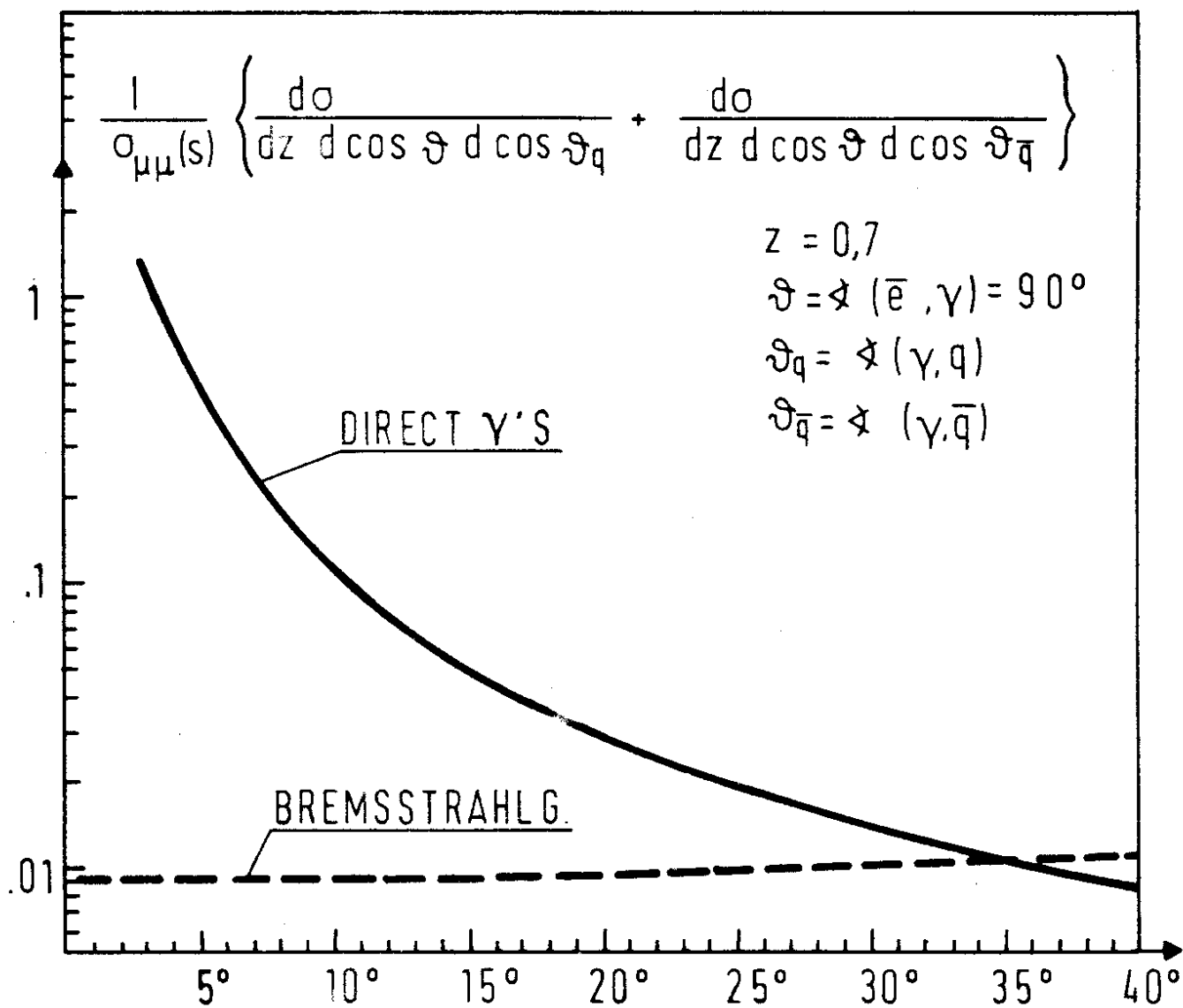


Fig. 9